Developmental Cell, Vol. 4, 119–129, January, 2003, Copyright ©2003 by Cell Press

The Forkhead Transcription Factor Foxo1 Regulates Adipocyte Differentiation

Jun Nakae,[1,3] Tadahiro Kitamura,[1] Yukari Kitamura,[1] William H. Biggs III,[2] Karen C. Arden,[2] and Domenico Accili[1,*]

[1]Naomi Berrie Diabetes Center
Department of Medicine
College of Physicians and Surgeons
of Columbia University
New York, New York 10032

[2]Ludwig Institute for Cancer Research
University of California, San Diego
La Jolla, California 92093

Summary

An outstanding question in adipocyte biology is how hormonal cues are relayed to the nucleus to activate the transcriptional program that promotes adipogenesis. The forkhead transcription factor Foxo1 is regulated by insulin via Akt-dependent phosphorylation and nuclear exclusion. We show that Foxo1 is induced in the early stages of adipocyte differentiation but that its activation is delayed until the end of the clonal expansion phase. Constitutively active Foxo1 prevents the differentiation of preadipocytes, while dominant-negative Foxo1 restores adipocyte differentiation of fibroblasts from insulin receptor-deficient mice. Further, *Foxo1* haploinsufficiency protects from diet-induced diabetes in mice. We propose that Foxo1 plays an important role in the integration of hormone-activated signaling pathways with the complex transcriptional cascade that promotes adipocyte differentiation.

Introduction

White adipose tissue plays an important metabolic role by storing triacylglycerol in periods of energy excess and releasing free fatty acids and glycerol during energy deprivation (Spiegelman and Flier, 2001). Furthermore, adipocytes secrete a number of hormones, collectively termed adipokines, that regulate metabolic homeostasis (Ahima and Flier, 2000). In rodents, brown adipose tissue has been implicated in thermogenesis. Increased fat deposition results in obesity, which, in turn, predisposes to type 2 diabetes, cardiovascular diseases, hypertension, sleep apnea, and musculoskeletal disorders (Spiegelman and Flier, 2001).

The process of adipocyte differentiation has been extensively characterized in cultures of clonal cell lines of preadipocytes, such as mouse 3T3-L1 and 3T3-F442A (Gregoire et al., 1998; Rosen et al., 2000). In vitro adipogenesis requires a sequence of events, including growth arrest of proliferating preadipocytes, coordinated reentry into the cell cycle with limited clonal expansion, and growth arrest associated with terminal differentiation. These processes are accompanied by characteristic changes in gene expression.

Insulin and insulin-like growth factor-1 promote differentiation of preadipocytes in vitro (Rubin et al., 1977). 3T3-L1 cells with partial inactivation of *Insulin Receptor* (*Insr*) display impaired adipocyte differentiation (Accili and Taylor, 1991), and *Insr* knockout mice have marked adipose tissue hypotrophy (Cinti et al., 1998). Moreover, embryonic fibroblasts (EF) with combined ablation of the insulin receptor substrates Irs1 and Irs2 fail to differentiate into adipocytes (Miki et al., 2001). Adipocyte differentiation is associated with a transient increase of PI 3-kinase activity (Sakaue et al., 1998) and can be induced by overexpression of a constitutively active form of Akt, one of the PI 3-kinase-activated kinases (Kohn et al., 1996). These data are consistent with a role of insulin-stimulated PI 3-kinase signaling in adipogenesis. However, the mechanism by which the PI 3-kinase → Akt signal is relayed to the nucleus to activate adipocyte differentiation is unknown.

Akt phosphorylates the Foxo transcription factors (Kaestner et al., 2000) and inhibits their transcriptional activity (Datta et al., 1999; Kops and Burgering, 1999). Foxo1 is the most abundant Foxo isoform in several insulin-responsive tissues, such as liver, adipose, and pancreatic β cells. We have shown that Foxo1 regulates *glucose-6-phosphatase* (Nakae et al., 2001) and *Pdx1* expression (Kitamura et al., 2002) and is involved in insulin inhibition of hepatic glucose production and stimulation of β cell proliferation (Nakae et al., 2002). In the present study, we investigated the role of Foxo1 in adipose tissue. Our data indicate that Foxo1 plays an important role in coupling insulin signaling to adipocyte differentiation.

Results and Discussion

Foxo Isoform Expression during 3T3-F442A Differentiation

In vitro differentiation of committed preadipocytes follows a well-characterized sequence: upon reaching confluence (day 0), cells undergo limited clonal expansion (days 1–2), postmitotic growth arrest (days 3–4), and terminal differentiation (days 4–10).

Real-time RT-PCR analysis (Figure 1A) indicates that *Foxo1* is the most abundant *Foxo* isoform in murine white and brown adipose tissue, with levels ~50% and 70% of those detected in liver (Nakae et al., 2002). In 3T3-F442A preadipocytes, mRNA levels of the three isoforms are comparably low (Figure 1B). However, during differentiation, *Foxo1* expression increases up to 6-fold over basal levels, peaking at day 4, to then partially decline, while *Foxo3* expression does not change significantly. *Foxo4* expression nearly doubles by the end of differentiation (Figures 1B and 1C). These data indicate that *Foxo1* shows a unique expression pattern among *Foxo*s during differentiation of 3T3-F442A cells.

*Correspondence: da230@columbia.edu

[3]Present address: Department of Pediatrics, Asahikawa Medical College, Asahikawa 078-8510, Japan.

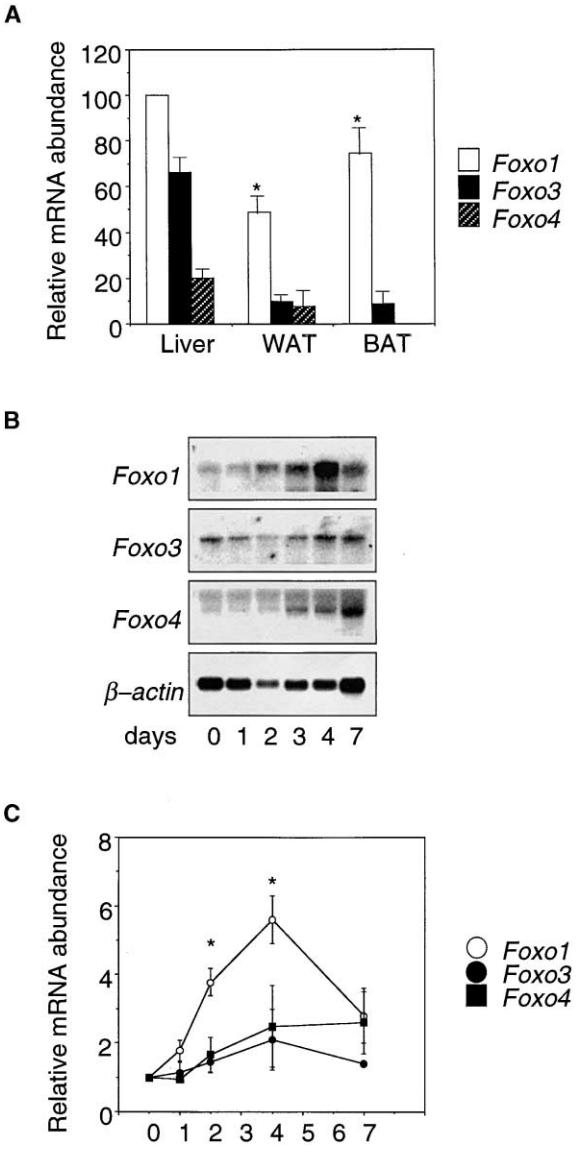

Figure 1. Expression of Foxo Isoforms in Adipose Tissue and during 3T3-F442A Adipocyte Differentiation

(A) Relative mRNA abundance of *Foxo1*, *3*, and *4* in liver, white adipose tissue (WAT), and brown adipose tissue (BAT). We analyzed 2-month-old mice ($n = 3$). A bar indicates the mean ±SEM. An asterisk indicates a significant difference between *Foxo1* and other *Foxo* isoforms ($p < 0.001$ by ANOVA).

(B) Representative experiment showing mRNA levels of Foxo isoforms in 3T3-F442A cells during differentiation. mRNA was hybridized sequentially with probes encoding *Foxo1* (top panel), *Foxo3* (second panel from the top), and *Foxo4* (third panel from the top) and normalized with β-actin (bottom panel).

(C) Summary of time-course analyses of Foxo isoform expression from several independent differentiation experiments. An asterisk indicates a significant difference at each time point between *Foxo1* and other *Foxo* isoforms ($p < 0.001$ by ANOVA).

Foxo1 Phosphorylation and Subcellular Localization during Adipocyte Differentiation

Foxo1 is regulated via phosphorylation by Akt and other PI-dependent kinases (Kops and Burgering, 1999). To study the regulation of Foxo1 phosphorylation during adipocyte differentiation, we measured immunoreactivity with a phosphospecific antibody against Ser^{253}, the main Akt phosphorylation site (Nakae et al., 2000). To this end, we transduced confluent 3T3-F442A cells with adenovirus encoding HA-tagged Foxo1. Phosphorylation of Ser^{253} was detectable at day 1, peaked at day 2, and returned to basal levels at day 3. Western blotting with anti-HA antibody shows that Foxo1 expression was constant during the experiment (Figure 2A). These data indicate that phosphorylation of Foxo1 is regulated in a stage-dependent manner.

We next investigated the subcellular distribution of Foxo1 during adipocyte differentiation by immunocytochemistry. Foxo1 was undetectable in preadipocytes (Figure 2B, day 0). At day 2, it was largely detected in a cytoplasmic localization. At day 4, it could be detected in a typical nuclear localization pattern, and, at day 10, it localized throughout the cell. Thus, these experiments indicate a correlation between phosphorylation and subcellular localization.

Here is a summary of these findings. *Foxo1* expression is activated in preadipocytes coincidentally with growth arrest and peaks at the onset of terminal differentiation. However, during the clonal expansion phase, Foxo1 is inactive because it is phosphorylated. Activation occurs before the onset of terminal differentiation, when Foxo1 becomes dephosphorylated and localizes to the nucleus. Interestingly, this is also the time when mRNA levels reach their maximal levels. These data suggest a requirement for Foxo1 during the transition from clonal expansion to terminal differentiation of preadipocytes, and they are consistent with Foxo1's role to induce cell cycle inhibitors, such as *p27* (Medema et al., 2000) and the retinoblastoma-like protein *p130* (Kops et al., 2002).

A Gain-of-Function Foxo1 Mutant Inhibits Adipocyte Differentiation

To investigate the role of Foxo1 in adipocyte differentiation, we transduced 3T3-F442A cells with four different adenoviral vectors encoding wild-type, constitutively active (ADA), or dominant-negative (Δ256) Foxo1, as well as LacZ as a control for adenoviral toxicity. The constitutively active Foxo1 carries mutations of the three main phosphorylation sites; as a result, it cannot be excluded from the nucleus in response to insulin (Nakae et al., 2001). The dominant-negative Foxo1 contains the forkhead DNA binding domain but lacks the transactivation domain. As a result, it is transcriptionally inactive and prevents DNA binding of endogenous Foxo1 (Nakae et al., 2001). We carried out adenoviral transduction at the time of induction of differentiation (48 hr postconfluence). Expression of wild-type Foxo1 and LacZ had no effect on adipocyte differentiation (data not shown). Expression of the Foxo1-ADA and Foxo1-Δ256 mutants was detected within one day of transduction and persisted for up to 7 days. The ADA mutant showed a peak of expression after 2 days, which was not observed with the Δ256 mutant (Figure 3A).

Expression of the Foxo1-ADA mutant resulted in a dose-dependent inhibition of adipocyte differentiation, as assessed by oil red O staining (Figure 3B) and by the reduced expression of *Pparγ* and *Glut4* 7 days postinduction (Figure 3C). Transduction of 3T3-F442A cells

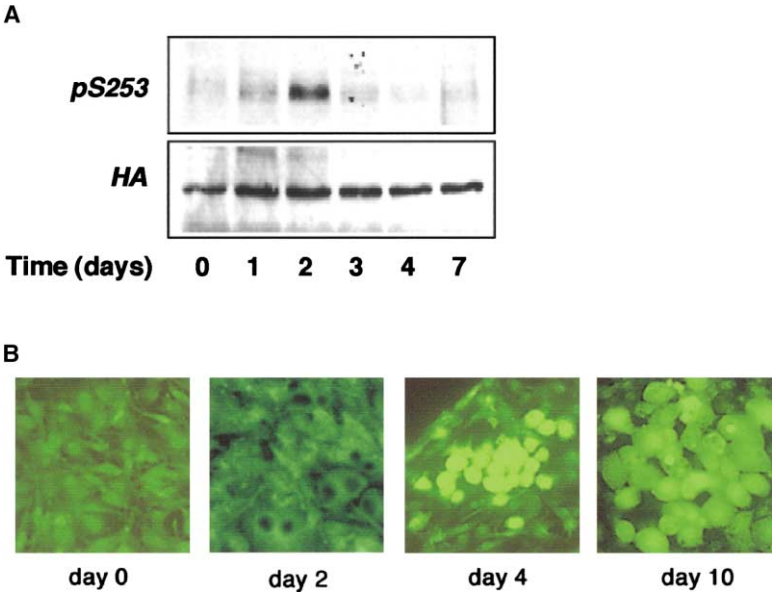

Figure 2. Phosphorylation and Subcellular Localization of Foxo1 in Differentiating Adipocytes

(A) Foxo1 phosphorylation in 3T3-F442A cells is regulated in a stage-dependent manner during differentiation. We transduced 3T3-F442A cells with HA-tagged wild-type Foxo1 one day prior to induction of differentiation. We collected cells at various time points during differentiation and performed sequential Western blotting with anti-pSer^{253} (top panel) and anti-HA antibodies (bottom panel). A representative experiment is shown.

(B) Detection of Foxo1 subcellular localization by immunocytochemistry. Cells were plated on chamber slides and fixed at different points during the differentiation process. We used anti-Foxo1 antiserum to detect the endogenous Foxo1 using immunofluorescence.

with the Foxo1-ADA mutant after clonal expansion did not affect adipogenesis. Likewise, transduction of fully differentiated cells did not result in dedifferentiation. These data indicate that ectopic nuclear expression of Foxo1 prior to terminal differentiation arrests adipose conversion of 3T3-F442A cells.

To identify Foxo1 target genes, we performed time-course analyses of mRNA expression in cells expressing the ADA mutant (Figure 3C). Expression of *C/EBP*β and *C/EBP*δ was prematurely induced and returned to basal levels by day 7. Interestingly, these two isoforms have been shown to induce Pparγ expression (Wu et al., 1999) but, in Foxo1-ADA-transduced cells, failed to do so. A potential explanation for this finding emerged from the analysis of *Chop10/Gadd153* expression. Chop10 is a member of the C/EBP family that lacks a DNA binding domain and is thought to inhibit C/EBP function via dimerization with the various isoforms (Batchvarova et al., 1995; Tang and Lane, 2000). In untransduced cells, *Chop10* expression was characteristically inhibited in the early phases of adipocyte differentiation and induced during terminal differentiation. The expression pattern of *Chop10* in cells transduced with the Foxo1-ADA mutant was reversed, with an early induction followed by a return to basal levels at the end of the differentiation phase.

Expression of the cell cycle control genes *pRb*, *p21*, and *p27* was strongly induced at day 2 and returned to normal thereafter. This induction coincided with peak levels of Foxo1-ADA expression. Expression of *Pparγ*, *Glut4*, *Acrp30* (Figure 3D), and *C/EBP*α (data not shown) was abrogated, consistent with the lack of adipose differentiation. The data are summarized in Figure 3D.

In contrast to the Foxo1-ADA mutant, transduction with Foxo1-Δ256 was associated with earlier induction of adipocyte differentiation (data not shown). This change was paralleled by an earlier induction of *Pparγ*, *Glut4*, and *Acrp30* expression, while expression of *C/EBP*β, *C/EBP*δ, *Chop10*, *p27*, *pRb*, and *p21* was unchanged (Figures 3C and 3D).

In summary, inhibition of adipocyte differentiation by the Foxo1-ADA mutant is associated with induction of the cell cycle inhibitors p21, p27, and pRb and the C/EBP dimerization partner Chop10 (Figure 3D). These findings are consistent with the possibility that Foxo1 inhibits adipocyte differentiation via a complex mechanism. On the one hand, Foxo1 appears to induce an early growth arrest, which could potentially prevent clonal expansion of committed preadipocytes; on the other hand, Foxo1 may directly inhibit C/EBP-dependent terminal differentiation via increased Chop10 expression.

Ectopic Expression of Dominant-Negative Foxo1 Restores Adipocyte Differentiation of EF Lacking Insulin Receptors

Since a constitutively active Foxo1 mutant inhibits adipocyte differentiation, we asked whether a dominant-negative mutant enhances adipogenesis. In 3T3-F442A cells, transduction with the Δ256 mutant results in earlier induction of adipocyte-specific genes and adipose conversion. Next, we asked whether the Foxo1-Δ256 mutant would be able to restore adipogenesis in EF from *Insr*$^{-/-}$ mice. We have previously shown that *Insr*$^{-/-}$ mice have hypotrophic adipose tissue (Cinti et al., 1998).

Similar to EF from *Irs1/Irs2* double knockout mice (Miki et al., 2001), *Insr*$^{-/-}$ EF failed to convert to adipocytes in the presence of insulin/dexamethasone/IBMX (Figure 4A) or Pparγ ligand (data not shown). In contrast, following transduction with the Δ256 mutant, *Insr*$^{-/-}$ EF partially differentiated into mature adipocytes in the presence of hormonal induction (Figure 4A) or Pparγ ligand (data not shown). Furthermore, Northern blotting analysis showed restored expression of adipocyte-specific genes in Δ256-transduced, compared with nontransduced, *Insr*$^{-/-}$ EF, while expression of cell cycle control and C/EBP genes had not been affected (Figure 4B). These data indicate that the Δ256 mutant can partially restore adipocyte differentiation.

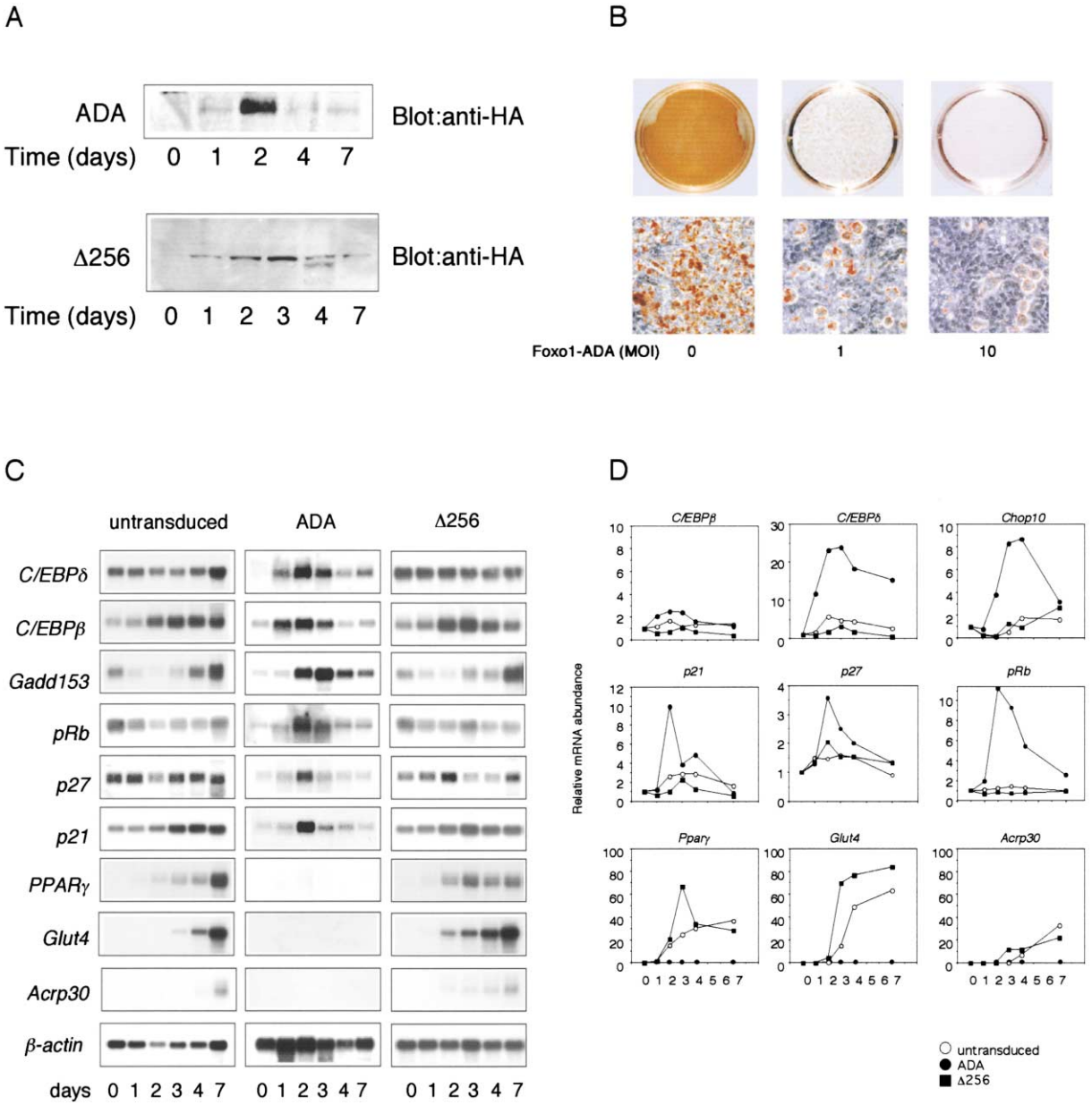

Figure 3. Inhibition of Adipocyte Differentiation by the Constitutively Active Mutant Foxo1-ADA

(A) Time-course analysis of adenoviral protein expression. Cells were transduced at day 0, and extracts were prepared at different time points. The Foxo1-ADA mutant is shown in the upper panel, and Foxo1-Δ256 mutant is shown in the lower panel. Equal amounts of protein extract were applied to each lane. The lower band observed at day 4 in Δ256-transduced cells is a dephosphorylated form of Foxo1.

(B) Effect of the constitutively active mutant Foxo1-ADA on adipocyte differentiation. The mutant protein was expressed with different moi of crude adenoviral preparations. We carried out transduction on the day of induction (i.e., 48 hr postconfluence). After removal of the adenoviral extract, cells underwent the regular differentiation protocol. The extent of adipocyte differentiation was determined by oil red O staining.

(C) Time-course analysis of gene expression in nontransduced 3T3-F442A cells (left panels) or after transduction with Foxo1-ADA (middle panels) or Foxo1-Δ256 (right panels).

(D) Quantification of relative mRNA abundance in 3T3-F442A cells during differentiation. Expression of each mRNA was quantified by scanning densitometry of the autoradiogram and normalized with β-actin.

Mechanisms of Foxo1 Regulation of Adipogenesis

The ability of Foxo1 to prevent adipose differentiation is associated with increased expression of cell cycle inhibitors and of the C/EBP modulator Chop10. We sought to identify bona fide Foxo1 targets among these genes. Although others have shown (Medema et al., 2000), and our present data confirm, that *p27* expression increased in Foxo1-transduced cells, the increase in *p27* expression was not paralleled by changes in protein levels (Figure 4C), and p27 gradually declined during differentiation. Moreover, cells transduced with the Δ256 mutant showed persistent p27 expression, suggesting that alterations of p27 levels are not responsible for the inhibitory effect of the constitutively active Foxo1

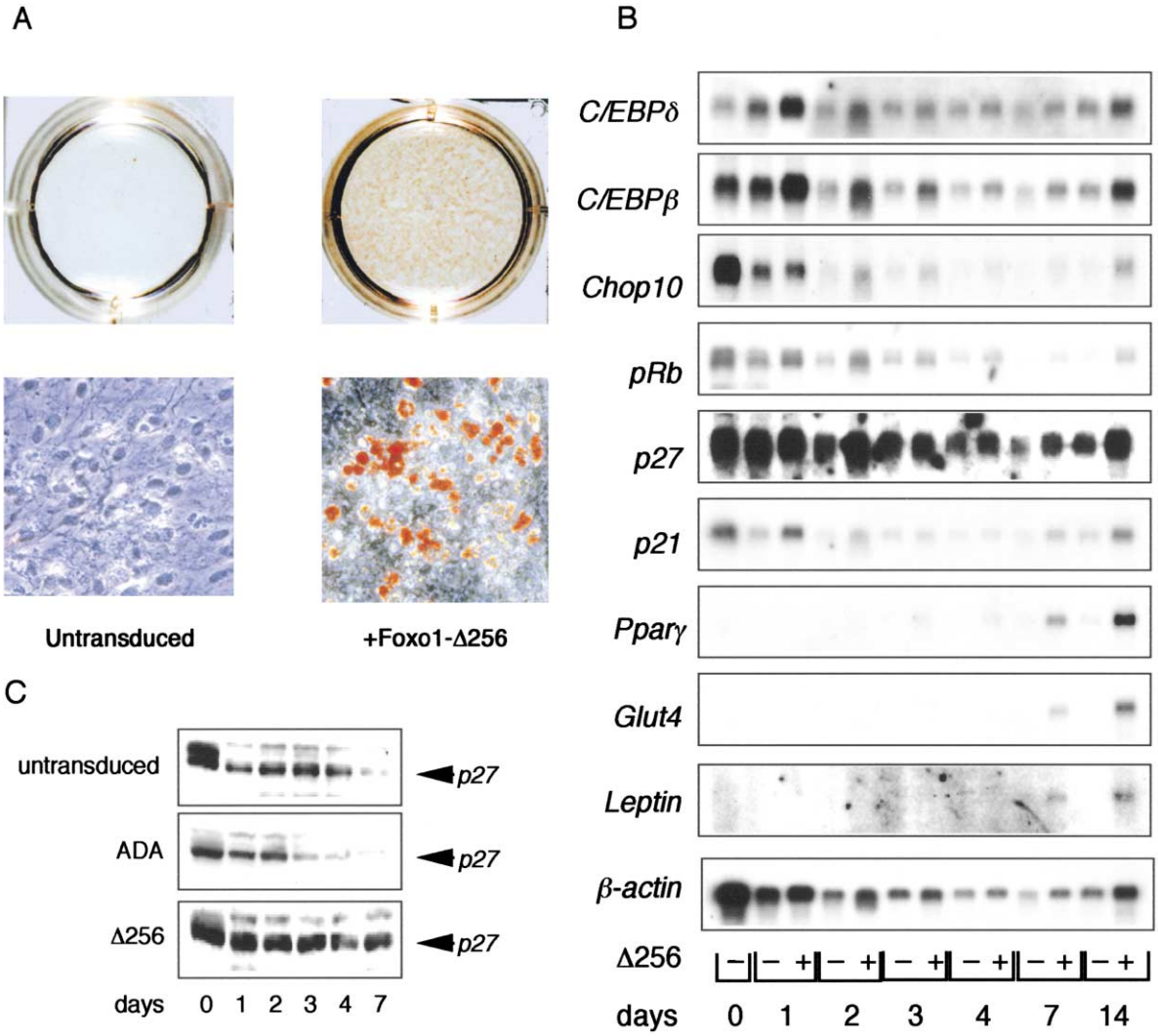

Figure 4. The Dominant-Negative Foxo1-Δ256 Restores Adipocyte Differentiation in EF from *Insr*$^{-/-}$ Mice

(A) Oil red O staining in nontransduced cells (left panel) or in Δ256-transduced (right panel) cells. Cells were grown to confluence and incubated with insulin/dexamethasone/IBMX to induce differentiation. They were stained with oil red O to assess triglyceride accumulation at day 14 postinduction.

(B) Time-course analysis of gene expression in *Insr*$^{-/-}$ EF in the absence (−) and presence (+) of the Foxo1-Δ256 mutant.

(C) Analysis of p27 protein expression by immunoblotting with anti-p27 antibody of extracts from nontransduced cells (upper panel) or cells transduced with Foxo1-ADA (middle panel) and Foxo1-Δ256 (lower panel). Cells were harvested at the indicated time points during differentiation.

mutant. Moreover, Foxo1 has been shown to induce cell cycle arrest of *p27*$^{-/-}$ fibroblast, suggesting that p27 is not required for the effects of Foxo1 on cell cycle progression (Kops et al., 2002).

Since p21 has been implicated in the termination of clonal expansion (Morrison and Farmer, 1999), we next investigated its regulation by Foxo1. Inspection of the mouse *p21* promoter region revealed several potential Foxo1 binding sites (AAAC/TA) in a tandem repeat arrangement between nucleotides (nt) –1337 and –1395 and nt –2596 and –2638. In cotransfection experiments, wild-type Foxo1 increased luciferase activity mediated through the *p21* promoter by ~4-fold ($p < 0.001$ by ANOVA) (Figure 5A). Addition of insulin resulted in an ~25% inhibition of Foxo1-dependent transcription. In contrast, *p21* reporter gene expression induced by the constitutively active Foxo1-ADA mutant was paradoxically stimulated in the presence of insulin. The dominant-negative mutant Foxo1-Δ256 suppressed *p21*-mediated reporter gene expression (Figure 5A). Expression levels of wild-type and Foxo1-ADA were similar (Figure 5B). To investigate whether Foxo1 can regulate expression of the endogenous *p21*, we transduced LLC kidney epithelial cells and SV40-transformed hepatocytes with the Δ256 or ADA mutants and measured *p21* mRNA. The ADA mutant increased *p21* expression by 65% compared with nontransduced LLC cells. The rise in *p21* mRNA levels was suppressed in a dose-dependent manner by the Δ256 mutant (Figure 5C). In cultured hepatocytes, the Foxo1-ADA mutant increased *p21*

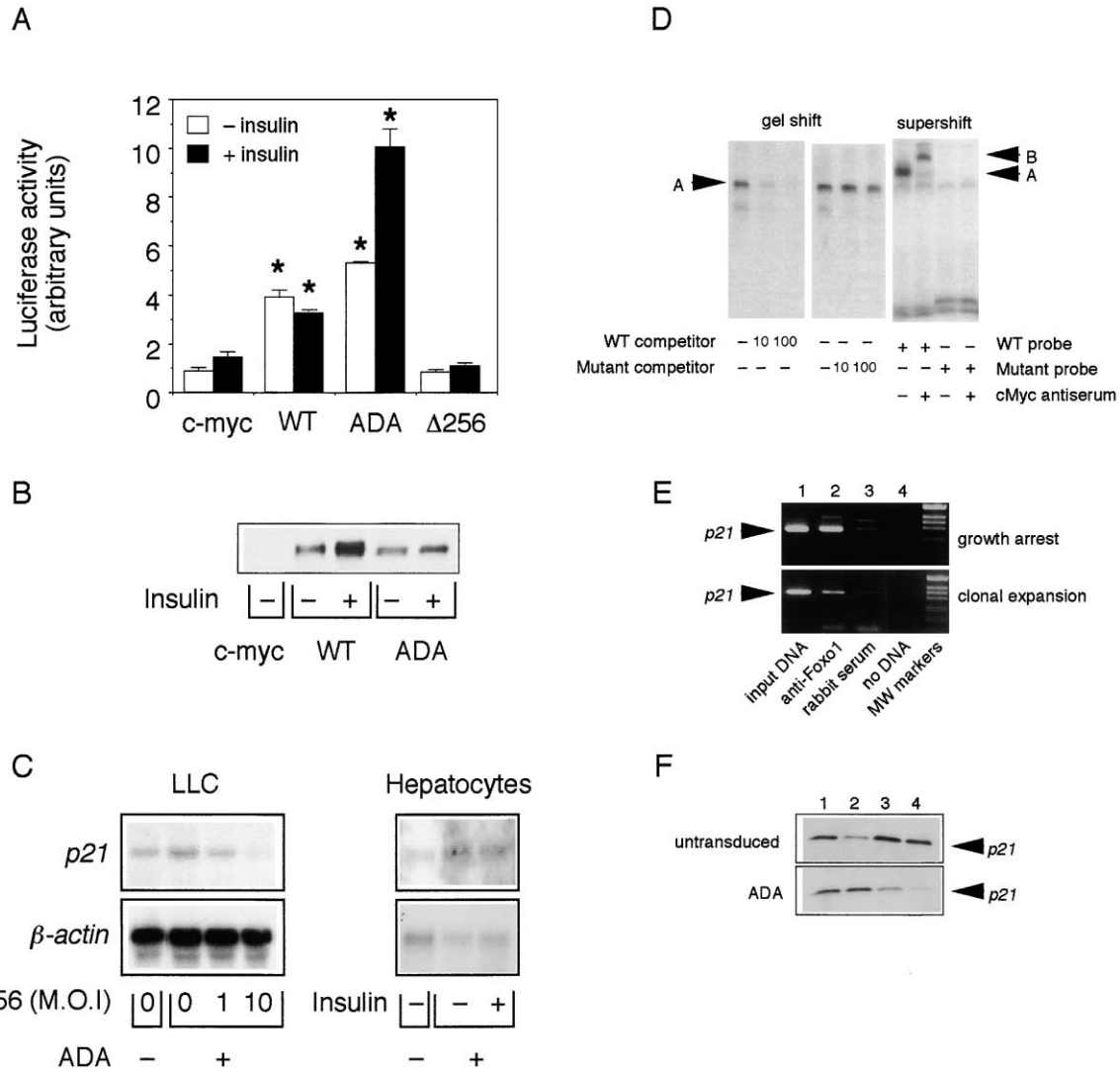

Figure 5. Foxo1 Regulates the p21 Promoter in an Insulin-Inhibitable Manner

(A) Expression of a p21-luciferase reporter gene in SV40-transformed hepatocytes. Cells were transiently cotransfected with wild-type or mutant Foxo1 (ADA and Δ256) and a *p21*-luciferase reporter construct. Twenty-four hours after transfection, some cells were treated with insulin (full bars). We used β-galactosidase to normalize luciferase activity for transfection efficiency. A bar represents the mean ±SEM of three experiments. An asterisk on the empty bars indicates a significant difference between mock-transfected (empty vector) and Foxo1-transfected cells ($p < 0.001$ by ANOVA). An asterisk on the full bars indicates a significant difference between insulin-treated cells and basal luciferase activity in the same experiment ($p < 0.05$ by ANOVA).

(B) Expression of cMyc-tagged Foxo1 wild-type and ADA mutant was determined by immunoblotting with anti-Foxo1 antiserum in total cell extracts after transient transfection.

(C) Effect of constitutively active and dominant-negative Foxo1 mutants on endogenous *p21* mRNA in kidney epithelial LLC cells (left panel) and SV40-transformed hepatocytes (right panel). LLC cells were transduced with the Δ256 mutant at increasing moi, in the absence or presence of a fixed amount of Foxo1-ADA. SV40-transformed hepatocytes were transduced with Foxo1-ADA and treated with insulin.

(D) Gel shift assays. Oligonucleotide probes corresponding to the forkhead binding site at nt 1369–1395 of the *p21* promoter were incubated with nuclear extracts in the absence or presence of increasing amounts of unlabeled control or mutant oligo (left panel). In the right panel, anti-cMyc antiserum was added to the reaction mix containing the wild-type or mutant probe. The position of the gel-retarded complex is indicated as A, and that of the super-shifted complex is indicated as B.

(E) Chromatin immunoprecipitation assays. We incubated crosslinked chromatin from cells at the indicated differentiation stages with anti-Foxo1 antiserum (lane 2) or control serum (lane 3). We analyzed the immunoprecipitated DNA with PCR primers to amplify the p21 promoter sequence. As controls, we show PCR reactions with total input chromatin (lane 1) and without added DNA (lane 4).

(F) Analysis of p21 protein expression by immunoblotting with anti-p21 antibody of extracts from nontransduced cells (upper panel) or cells transduced with Foxo1-ADA (lower panel). Cells were harvested at the indicated time points during differentiation.

expression 4-fold compared with nontransduced hepatocytes. This induction was unaffected by insulin treatment (Figure 5C). These data indicate that Foxo1 regulates *p21* transcription.

We next analyzed Foxo1's ability to bind the *p21* promoter in gel shift and chromatin immunoprecipitation (ChIP) assays. Incubation of nuclear extracts from cells expressing cMyc-tagged Foxo1 with a probe encoding

the forkhead binding site between nt –1369 and –1395 in the *p21* promoter yielded a gel-retarded complex that could be competed by excess cold probe, but not by a mutant probe. Complex A was super shifted by the addition of anti-cMyc antiserum to yield complex B (Figure 5D). We detected no binding to the mutant probe and weak binding to the second forkhead site (nt –1337 to –1367; data not shown). These data indicate that Foxo1 can bind to the *p21* promoter and regulate its expression in an insulin-inhibitable manner.

ChIP assays provided evidence that the interaction between Foxo1 and the *p21* promoter occurs in vivo in a stage-specific fashion. In crosslinked chromatin isolated from cells during clonal expansion and immunoprecipitated with anti-Foxo1 antiserum, we detected an amplified product corresponding to the p21 promoter, with only trace amounts of nonspecific binding to control serum (Figure 5E). The intensity of the amplified signal declined by ~80% in cells undergoing terminal differentiation, consistent with a decrease in Foxo1 binding, as might have been expected on the basis of the nuclear exclusion of Foxo1 at this stage.

Changes in p21 protein levels, measured by Western blotting with anti-p21 antiserum in cells transduced with ADA or D256 mutants, mirrored the changes in mRNA levels. Thus, in untransduced 3T3-F422A cells, p21 levels declined during clonal expansion (Figure 5F, compare lanes 1 and 2). In contrast, p21 levels increased in ADA-expressing cells.

The *Chop10* promoter also contains potential forkhead bindings sites. However, in transient transfection experiments, Foxo1 failed to affect *Chop10* promoter activity, suggesting that the changes in *Chop10* expression are not a direct result of Foxo1 binding to its promoter (data not shown).

In summary, from this analysis, we identified the cell cycle inhibitor *p21* as a bona fide Foxo1 target with a potential role in Foxo1 control of adipogenesis. The role of p27 in Foxo1-dependent adipogenesis remains unclear. Recently, it has been suggested that overexpression of Wnt may also block adipogenesis by preventing the downregulation of p27 that is associated with clonal expansion (Ross et al., 2002). However, in view of the fact that cells expressing the dominant-negative Foxo1-Δ256 undergo robust differentiation and fail to downregulate p27 expression, it appears that p27 is not the mediator of Foxo1's effect on adipogenesis.

Foxo1 Haploinsufficiency Prevents Insulin Resistance and Diabetes Induced by a High-Fat Diet

To investigate the role of Foxo1 in adipose tissue in vivo, we analyzed the effects of *Foxo1* haploinsufficiency in a model of diet-induced diabetes. We have previously shown that *Foxo1* haploinsufficiency restores insulin sensitivity in insulin-resistant mice ($Insr^{+/-}$) by a complex mechanism involving decreased hepatic glucose production, increased pancreatic β cell compensation, and increased expression of insulin-sensitizing genes in adipose tissue (Nakae et al., 2002). When $Foxo1^{+/-}$ mice were fed a high-fat diet, they gained weight to the same extent as wild-type littermates (Figure 6A). However, unlike wild-type littermates, some of which developed diabetes (defined as whole blood glucose values greater than the mean plus 2 SD on two separate occasions), all $Foxo1^{+/-}$ mice remained euglycemic (Figures 6B and 6C). Moreover, wild-type mice rapidly developed hyperinsulinemia, consistent with insulin resistance. In contrast, $Foxo1^{+/-}$ mice developed hyperinsulinemia only at the end of the treatment period and to a significantly lower extent than wild-type controls (Figure 6D).

A metabolic characterization of high-fat-fed mice confirmed the protective effect of Foxo1 haploinsufficiency against diet-induced insulin resistance and diabetes. Thus, wild-type mice showed abnormal glucose (Figure 6E) and insulin tolerance (Figure 6F) at the end of the experiment. $Foxo1^{+/-}$ mice showed a mild, nonsignificant deterioration of glucose tolerance (Figure 6E) and no change in insulin tolerance (Figure 6F).

We next analyzed size, cellular composition, and gene expression in epididymal fat pads. The weight of epididymal fat pads nearly doubled in both genotypes after 15 weeks of high-fat diet (Figure 7A). The increase in size was associated with increased cell size in wild-type mice. In contrast, cell size was unchanged in $Foxo1^{+/-}$ mice (Figure 7B). Fat cell density decreased in high-fat-fed wild-type mice but remained constant in $Foxo1^{+/-}$ mice (Figure 7C), suggesting that *Foxo1* haploinsufficiency prevents adipocyte hypertrophy in response to high-fat feeding. Interestingly, *Foxo1* haploinsufficiency had a similar effect to reduce adipocyte size in insulin-resistant $Insr^{+/-}$ mice (data not shown).

We analyzed expression of several genes involved in adipocyte metabolism using real-time RT-PCR. In wild-type mice, expression of *Pparγ*, *Glut4*, *Leptin*, *Acrp30*, and *Srebp-1c* decreased ~75% following a high-fat diet. No changes were observed in the expression of *Tnfα* and *Resistin* (Figure 7D, empty circles). In $Foxo1^{+/-}$ mice, we observed a modest decrease of *Pparγ*, whereas *Glut4* levels rose slightly. *Leptin*, *Acrp30*, and *Srebp-1c* levels were lower in $Foxo1^{+/-}$ mice on normal chow than in wild-type mice and did not change following the high-fat diet. Moreover, we observed a decrease in *Tnfα* and *Resistin* levels (Figure 7D, filled circles).

These data demonstrate a protective effect of *Foxo1* haploinsufficiency against the deterioration of insulin sensitivity associated with diet-induced obesity. In addition to preserved fuel metabolism, $Foxo1^{+/-}$ mice showed none of the changes in gene expression that would predispose to insulin resistance in the fat cell. Notably, *Pparγ* expression did not change, and expression of two adipokines— *Tnfα* and *Resistin*—paradoxically decreased in high-fat-fed $Foxo1^{+/-}$ mice.

Conclusions

The data presented shed light onto two unresolved issues in adipocyte biology: the mechanism by which hormonal signaling activates transcriptional responses and the complex relationship between cell cycle control and induction of adipogenesis.

There are some precedents for regulation of adipogenesis through phosphorylation of transcription factors. For example, activation of MAP kinase has been shown to inhibit adipogenesis through Pparγ phosphorylation (Hu et al., 1996), while the stress-activated kinase

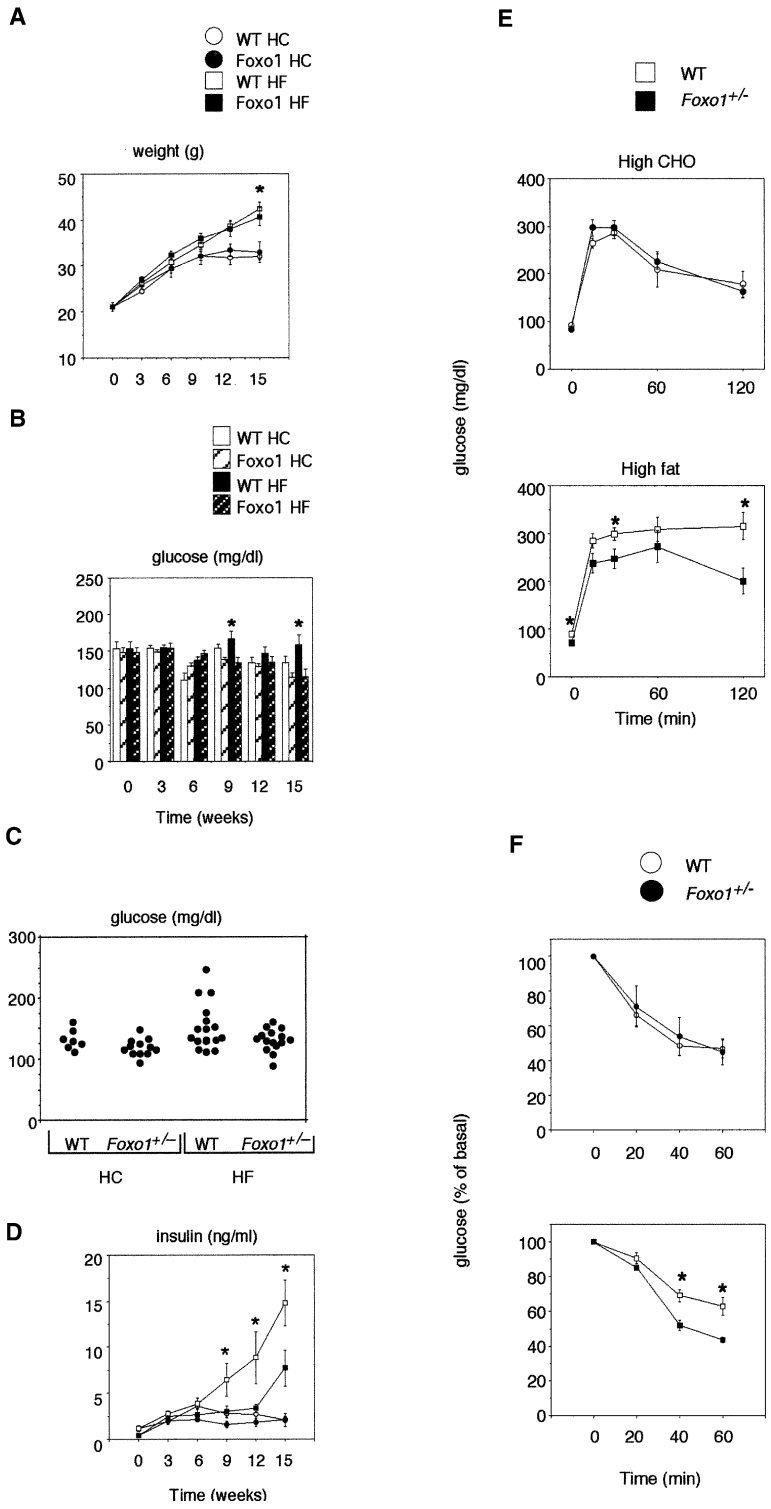

Figure 6. *Foxo* Haploinsufficiency Protects against Diet-Induced Diabetes

(A) *Foxo1*$^{+/-}$ mice and wild-type littermate controls were fed either regular, high-carbohydrate (HC) chow or a high-fat diet (HF) starting at weaning for a 15 week period. Body weights were measured at 3 week intervals (n = 8 wt and 12 *Foxo1*$^{+/-}$ on the control HC diet and 17 wt and 18 *Foxo1*$^{+/-}$ on the HF diet).

(B and C) Glucose levels in the fed state. The mean values ±SEM are indicated in (B), and individual values are shown in (C). Mice with glucose values greater than the mean plus 2 SD on two or more occasions were considered diabetic.

(D) Insulin levels were measured in random-fed animals at the indicated time points during the 15 week experiment.

(E and F) Metabolic characterization of high-fat-fed mice. Intraperitoneal glucose (E) and insulin tolerance (F) tests were performed as described previously (n = 10 for each genotype and each experimental condition). An asterisk indicates that $p < 0.01$ by ANOVA.

p38 inhibits adipogenesis via increased Chop10 phosphorylation (Wang and Ron, 1996). However, it is not known how insulin-induced protein phosphorylation is linked to the activation of adipogenesis. The present data provide a direct link between insulin signaling through Irs → PI 3-kinase → Akt and adipogenesis through Foxo1 phosphorylation. Inhibition of Foxo1 via phosphorylation appears to be required during the clonal expansion phase, and our data show that unrestrained Foxo1 activity prevents terminal differentiation.

These observations also appear to support the view that clonal expansion is a requirement for terminal differentiation. The antiadipogenic effect of the Foxo1-ADA mutant is associated with marked induction of several

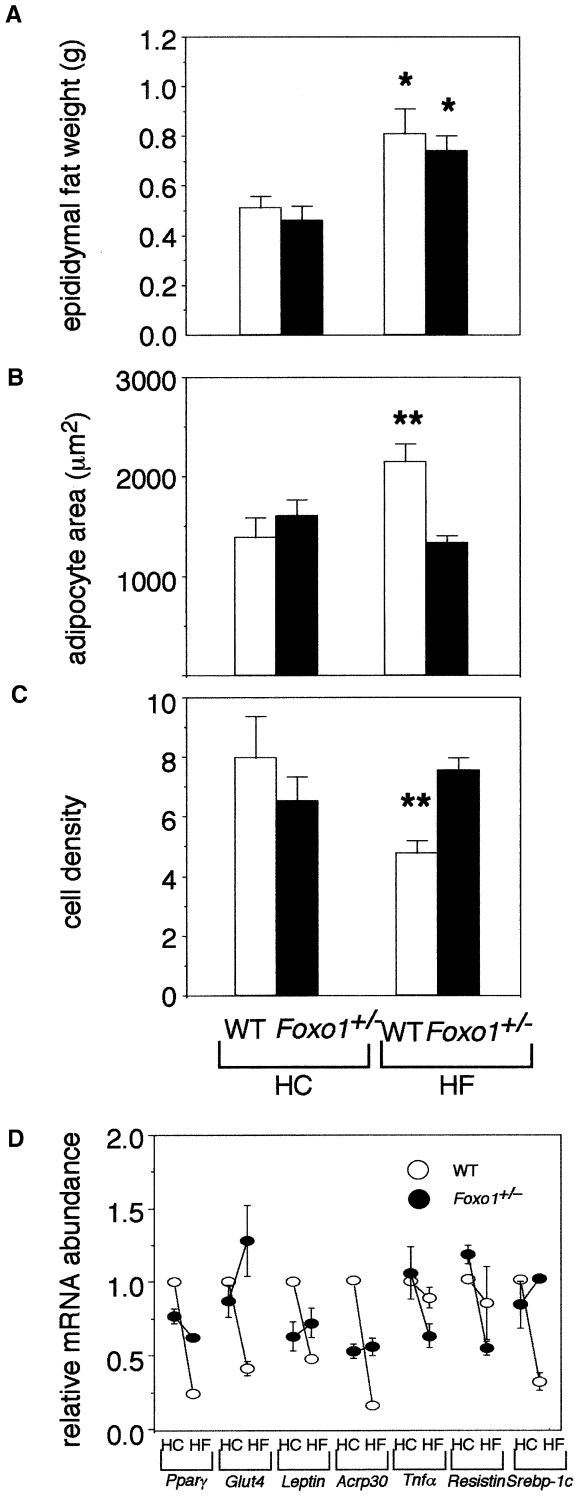

Figure 7. *Foxo1* Haploinsufficiency Protects against Increased Adipocyte Size and Changes in Adipocyte Gene Expression in Mice Fed a High-Fat Diet

(A) Epididymal fat weight in wild-type (empty bars) and *Foxo1*$^{+/-}$ mice (full bars) (n = 10 each), after 15 weeks of either HC or HF diet.

(B) Adipocyte size in epididymal fat pads was determined by morphometric analyses of hematoxylin- and eosin-stained adipose tissue sections. At least 500 cells were evaluated in six mice for each genotype.

(C) The number of fat cells within a random microscopic field was determined by counting cells in at least six different random fields per mouse and six mice for each genotype and treatment group. An asterisk indicates a significant difference ($p < 0.05$ by ANOVA) between wild-type and *Foxo1*$^{+/-}$ mice.

(D) Gene expression in epididymal fat samples was determined by RT-PCR in three mice for each genotype. Each PCR was carried out in triplicate. For each gene, we report the values in control (HC) and high-fat-fed (HF) mice.

cell cycle inhibitors, including p21, pRb, and p27. The regulation of *p21* by Foxo1 represents a potential mechanism to explain the observed effects. The increase in p21 expression induced by Foxo1-ADA could prevent adipocyte differentiation by inhibiting clonal expansion. The notion that p21 is regulated by Foxo1 changes our understanding of this key step in adipocyte differentiation. In fact, it has been shown that p21 expression can be regulated in a Ppar ligand-dependent manner in cells expressing Pparγ (Morrison and Farmer, 1999). These data, along with the demonstrated ability of both C/EBPs and Pparγ to induce growth arrest of preadipocytes, have generally been interpreted as supporting the view that Ppar is upstream of p21 in the process of adipocyte differentiation (Spiegelman and Flier, 2001). However, in cells expressing Foxo1-ADA, increased p21 expression is dissociated from Pparγ induction, raising the possibility that control of p21 expression is exerted upstream of Pparγ by Foxo1. The complex relationship among Foxo1, p21, C/EBP, and Pparγ deserves further investigation.

Interestingly, we found that Foxo1 also binds to forkhead sites of the Rb promoter in gel shift assays (data not shown), suggesting that Rb is also a Foxo1 target. The role of Rb in adipocyte differentiation and its interaction with the C/EBP and Ppar transcription factors is underscored by the observation that *Rb*$^{-/-}$ EF fail to differentiate into adipocytes (Chen et al., 1996) but can be rescued by Pparγ ligands (Hansen et al., 1999). Moreover, the pRb target E2F has been shown to regulate clonal expansion of preadipocytes (Fajas et al., 2002). Thus, it is possible that Foxo1 controls adipocyte differentiation through interactions with several genes involved in progression through the cell cycle. Interestingly, a similar phenotype has been observed in preadipocytes overexpressing Wnt (Ross et al., 2002), raising the possibility that Wnt signaling and Foxo1 signaling may be hierarchically related or share a common set of target genes. More work will be required to address these questions.

Foxo1 overexpression leads to a remarkable alteration in Chop10 expression patterns during adipocyte differentiation. However, since we have been unable to demonstrate direct control of the *Chop10* promoter by Foxo1, it is possible that altered *Chop10* expression is solely a result of Foxo1 inhibition of cell cycle progression. Alternatively, Foxo1 could promote expression of another protein that regulates Chop10.

Finally, analysis of mice with Foxo haploinsufficiency is consistent with an in vivo role of Foxo1 in the process of adipocyte differentiation. The regulation of adipocyte differentiation by Foxo1 can potentially affect insulin sensitivity by regulating adipocyte size. Inhibition of

Foxo1 function holds promise as a therapeutic approach to insulin resistance and diabetes.

Experimental Procedures

mRNA Isolation, Northern Blotting, and Real-Time RT-PCR

We performed mRNA isolation and Northern hybridization according to standard techniques. We carried out real-time RT-PCR on pooled samples from three 2-month-old mice using a Roche LightCycler PCR instrument and LightCycler SYBR Green I (Roche Perkin-Elmer) RNA amplification kit. Each reaction was carried out in triplicate under standard reaction conditions. Primer sequences used to amplify *Foxo1*, *Foxo3*, *Foxo4*, *Pparγ*, *Glut4*, *Leptin*, *Acrp30*, *Tnfα*, *Resistin*, *Srebp-1c*, and β-actin are available upon request.

Cell Culture and Induction of Adipocyte Differentiation

3T3-F442A preadipocytes were maintained in DMEM containing 25 mM glucose and supplemented with 10% calf serum, 2 mM L-glutamine, 50 U/ml penicillin, and 50 μg/ml streptomycin. Forty-eight hours after cells had reached confluence, we induced adipocyte differentiation by adding insulin (5 μg/ml) to the culture medium for 24 hr. In vitro differentiation was detected by staining cells with oil red O solution (0.5% in isopropyl alcohol solution-distilled water 60:40) for 30 min and then washing three times with distilled water.

LLC cells and SV40-transformed hepatocytes were cultured as described (Nakae et al., 2001).

Preparation of EF from Insr$^{-/-}$ Mice and Induction of Adipocyte Differentiation

We set up intercrosses of *Insr*$^{+/-}$ mice to recover embryos at day E13.5. We dissected embryos from the uterus and extraembryonic membranes, minced them into small pieces, and incubated them for 30 min in 4 ml of 0.25% trypsin-EDTA solution at 37°C. We stopped the reaction by adding DMEM supplemented with 10% FCS, 50 U/ml penicillin, and 50 μg/ml streptomycin. We resuspended cell aggregates by pipetting and plated them on 15 cm culture dishes. After 2 days, we trypsinized cells, replated them on 12-well dishes, and cultured them in the same medium. Two days after cells achieved confluence, we replaced the medium with AMEM supplemented with 10% FCS, 50 U/ml penicillin, 50 μg/ml streptomycin, 0.5 mM IBMX, 1 μM dexamethasone, and 5 μg/ml insulin for induction of differentiation. We genotyped embryos as described (Kido et al., 2000).

Transduction of Constitutively Active and Dominant-Negative Foxo1

We have described adenoviral vectors encoding wild-type, constitutively active (ADA), and dominant-negative (Δ256) mutant Foxo1 in previous publications (Nakae et al., 2001). We transduced cells 2 days after confluence by incubating them with adenoviral preparations at different moi for 4 hr.

Western Blotting and Immunoprecipitation

We homogenized tissues in buffer containing 10 mM HEPES (pH 7.6), 1.5 mM $MgCl_2$, 0.5 mM DTT, 10 mM KCl, 10 mM NaF, 1 mM Na_3VO_4, and 0.5 mM PMSF. After 15 min at 4°C, we added NP-40 to a final concentration of 2%. Following centrifugation (12,000 rpm for 1 min at 4°C), we resuspended the pellet in nuclear lysis buffer containing 20 mM HEPES (pH 7.5), 25% glycerol, 420 mM NaCl, 0.2 mM EDTA, 0.5 mM DTT, 10 mM NaF, 1 mM Na_3VO_4, 0.5 mM PMSF, 1% Triton X-100, 1% sodium deoxycholate, and 0.1% SDS (Nakae et al., 2002). After centrifugation to remove insoluble material, we processed a 50 μg aliquot for electrophoresis and Western blotting as described, using anti-Foxo1 antibody (H128, Santa Cruz), anti-phosphoSer^{253} Foxo1 antibody (Cell Signaling), anti-HA monoclonal antibody (12CA5; Boehringer Mannheim), anti-p27 monoclonal antibody (BD Transduction Laboratories), or anti-p21 monoclonal antibody (PharMingen).

Promoter Assays

We amplified the mouse p21 promoter using primers 5′-ggaagctta gacttccacccccatcaca-3′ (nt 2671–2691) and 5′-ggaagctttgagac gaggcctcgctatgt-3′ (nt 3381–3361; GenBank accession number U24171). We cloned the amplified products into the HindIII site of pGL3basic vector (Promega). We confirmed the identity of the cloned products by DNA sequencing. The day prior to transfection, we plated SV40-transformed hepatocytes onto 6-well plates. We performed transfections on 80% confluent cells using 1.5 μg of cMyc-tagged Foxo1 plasmid (wild-type, ADA, or Δ256) and 2 μg of pGL3B/p21. We used plasmid pRSV-β-galactosidase (20 ng) as an internal control of transfection efficiency. After transfection, we incubated cells in complete AMEM for 24 hr. Thereafter, we replaced medium with serum-free AMEM containing 0.1% bovine serum albumin with or without insulin (100 nM) and incubated it for 16 hr. We performed luciferase and β-galactosidase assays as described previously (Nakae et al., 2001).

Gel Shift Assays

We isolated nuclei from SV40-transformed mouse hepatocytes by sequential extraction in NaCl (Schreiber et al., 1989). We used two oligonucleotide probes: probe A (5′-gaggaatttgtttttgttttagaggca-3′; nt –1369 to –1395 in AF457187) and probe B (5′-aaaatttttgtttgtgtttgtt tcgagagag-3′; nt –1337 to –1367). We incubated double-stranded ^{32}P-labeled oligonucleotide probes (20,000 cpm, 5 fmol), corresponding to the consensus forkhead binding sites in the *p21* promoter, with nuclear extracts for 20 min at room temperature in the presence of 10 mM Tris-HCl (pH 7.5), 50 mM NaCl, 1 mM $MgCl_2$, 0.5 mM EDTA, 4% glycerol, 0.5 mM DTT, and 100 ng of poly(dI-dC). We resolved the DNA/protein complexes on 6% nondenaturing polyacrylamide gel and visualized them by autoradiography. For super shift experiments, we incubated anti-Foxo1 or nonimmune sera with nuclear extracts for 10 min at room temperature. We incubated competitor wild-type and mutant probes in the reaction mixture for 10 min prior to the addition of the radiolabeled probe.

Chromatin Immunoprecipitation Assays

We treated cultures of 3T3-F422A cells at various stages of differentiation with 1% formaldehyde for 10 min at room temperature and rinsed them in PBS. Thereafter, we lysed cells in buffer containing 1% SDS, 10 mM EDTA, 50 mM Tris-HCl (pH 8.1), and protease inhibitors (Roche) and sonicated samples using a Sonic Dismembrator (Model 550; Fisher) at maximal power setting with 20, 10 s pulses at 4°C. Following centrifugation, we diluted the lysates 1:10 in buffer containing 1% Triton X-100, 2 mM EDTA, 20 mM Tris-HCl (pH 8.1), and 150 mM NaCl and precleared them with 40 μl of salmon sperm DNA/protein A-Sepharose for 2 hr at 4°C. After removal of the Sepharose beads by centrifugation, we performed immunoprecipitation with anti-Foxo1 antiserum or an equal amount of normal rabbit IgG (Santa Cruz Biotechnology) for 1 hr at 4°C and then precipitation of the antibody-protein-DNA complexes with salmon sperm DNA/protein A-Sepharose. We washed the precipitates sequentially in buffers containing 0.1% SDS, 1% TritonX-100, 2 mm EDTA, and 20 mM TrisHCl (pH 8.1) supplemented with either 150 mM (buffer I) or 500 mM NaCl (buffer II) prior to a final wash in 250 mM LiCl, 1% NP-40, 1% deoxycholate, 1 mM EDTA, and 10 mM TrisHCl (pH 8.1). We washed the pellets with TE buffer and extracted them with 1% SDS and 100 mM Na_2HCO_3. After heating at 66°C for 6 hr to release crosslinked DNA, we digested proteins with Proteinase K and purified DNA with QIAquick Spin Kit (Qiagen). We subjected the samples to PCR using the following primers: 5′-aactcacagcttctccaaagcagg-3′ and 5′-catgtatgaagccaggagttggat-3′ (nt 1253–1276 and 1501–1524 of the *p21* promoter; GenBank accession number AF5457187). We employed standard reaction conditions and 25 cycles of amplification (Gerrish et al., 2001).

Immunofluorescence

We seeded 3T3-F442A cells into 4-well slide culture chambers (Lab Tek) and performed immunocytochemistry with anti-Foxo1 antibody at different time points during differentiation as described (Nakae et al., 2000).

Histological Analysis

We removed epididymal fat from 4- to 6-month-old mice, fixed the specimens in 10% paraformaldehyde, and embedded them in paraffin. We mounted consecutive 10 μm sections on slides and stained them with hematoxylin and eosin. We calculated adipose cell size

with the NIH Image 1.62 software by manual tracing of at least 500 adipocytes for each genotype.

High-Fat Diet

We have described previously the generation of *Foxo1*$^{+/-}$ mice (Nakae et al., 2002). Individually caged animals were fed either normal chow or high-fat diet beginning at weaning (3 weeks) for a 15 week period. The high-fat diet consisted of 45% of calories from fat, 35% from carbohydrate, and 20% from protein (Research Diets). Food consumption did not change among the various experimental groups.

Analytical Procedures

We measured glucose and insulin levels and performed glucose and insulin tolerance tests as described (Nakae et al., 2002). We performed descriptive statistics and analysis of variance (ANOVA) using the Stasview software (Abacus).

Acknowledgments

This work was supported NIH grants DK57539 and DK58282. We thank members of the Accili laboratory for critical discussion of the data and Prof. Kenji Fujieda (Asahikawa Medical College) for making his laboratory available to complete these studies.

Received: August 7, 2002
Revised: November 21, 2002

References

Accili, D., and Taylor, S.I. (1991). Targeted inactivation of the insulin receptor gene in mouse 3T3-L1 fibroblasts via homologous recombination. Proc. Natl. Acad. Sci. USA *88*, 4708–4712.

Ahima, R.S., and Flier, J.S. (2000). Adipose tissue as an endocrine organ. Trends Endocrinol. Metab. *11*, 327–332.

Batchvarova, N., Wang, X.Z., and Ron, D. (1995). Inhibition of adipogenesis by the stress-induced protein CHOP (Gadd153). EMBO J. *14*, 4654–4661.

Chen, P.L., Riley, D.J., Chen, Y., and Lee, W.H. (1996). Retinoblastoma protein positively regulates terminal adipocyte differentiation through direct interaction with C/EBPs. Genes Dev. *10*, 2794–2804.

Cinti, S., Eberbach, S., Castellucci, M., and Accili, D. (1998). Lack of insulin receptors affects the formation of white adipose tissue in mice. A morphological and ultrastructural analysis. Diabetologia *41*, 171–177.

Datta, S.R., Brunet, A., and Greenberg, M.E. (1999). Cellular survival: a play in three Akts. Genes Dev. *13*, 2905–2927.

Fajas, L., Landsberg, R.L., Huss-Garcia, Y., Sardet, C., Lees, J.A., and Auwerx, J. (2002). E2Fs regulate adipocyte differentiation. Dev. Cell *3*, 39–49.

Gerrish, K., Cissell, M.A., and Stein, R. (2001). The role of hepatic nuclear factor 1 alpha and PDX-1 in transcriptional regulation of the pdx-1 gene. J. Biol. Chem. *276*, 47775–47784.

Gregoire, F.M., Smas, C.M., and Sul, H.S. (1998). Understanding adipocyte differentiation. Physiol. Rev. *78*, 783–809.

Hansen, J.B., Petersen, R.K., Larsen, B.M., Bartkova, J., Alsner, J., and Kristiansen, K. (1999). Activation of peroxisome proliferator-activated receptor gamma bypasses the function of the retinoblastoma protein in adipocyte differentiation. J. Biol. Chem. *274*, 2386–2393.

Hu, E., Kim, J.B., Sarraf, P., and Spiegelman, B.M. (1996). Inhibition of adipogenesis through MAP kinase-mediated phosphorylation of PPARgamma. Science *274*, 2100–2103.

Kaestner, K.H., Knochel, W., and Martinez, D.E. (2000). Unified nomenclature for the winged helix/forkhead transcription factors. Genes Dev. *14*, 142–146.

Kido, Y., Burks, D.J., Withers, D., Bruning, J.C., Kahn, C.R., White, M.F., and Accili, D. (2000). Tissue-specific insulin resistance in mice with combined mutations of insulin receptor, IRS-1 and IRS-2. J. Clin. Invest. *105*, 199–205.

Kitamura, T., Nakae, J., Kitamura, Y., Kido, Y., Biggs, W., Wright, C., White, M., Arden, K., and Accili, D. (2002). The transcription factor Foxo1 links insulin signaling to Pdx1 regulation of pancreatic β-cell growth. J. Clin. Invest. *110*, 1839–1847.

Kohn, A.D., Summers, S.A., Birnbaum, M.J., and Roth, R.A. (1996). Expression of a constitutively active Akt Ser/Thr kinase in 3T3-L1 adipocytes stimulates glucose uptake and glucose transporter 4 translocation. J. Biol. Chem. *271*, 31372–31378.

Kops, G.J., and Burgering, B.M. (1999). Forkhead transcription factors: new insights into protein kinase B (c-akt) signaling. J. Mol. Med. *77*, 656–665.

Kops, G.J., Medema, R.H., Glassford, J., Essers, M.A., Dijkers, P.F., Coffer, P.J., Lam, E.W., and Burgering, B.M. (2002). Control of cell cycle exit and entry by protein kinase B-regulated forkhead transcription factors. Mol. Cell. Biol. *22*, 2025–2036.

Medema, R.H., Kops, G.J., Bos, J.L., and Burgering, B.M. (2000). AFX-like forkhead transcription factors mediate cell-cycle regulation by Ras and PKB through p27kip1. Nature *404*, 782–787.

Miki, H., Yamauchi, T., Suzuki, R., Komeda, K., Tsuchida, A., Kubota, N., Terauchi, Y., Kamon, J., Kaburagi, Y., Matsui, J., et al. (2001). Essential role of insulin receptor substrate 1 (IRS-1) and IRS-2 in adipocyte differentiation. Mol. Cell. Biol. *21*, 2521–2532.

Morrison, R.F., and Farmer, S.R. (1999). Role of PPARgamma in regulating a cascade expression of cyclin- dependent kinase inhibitors, p18(INK4c) and p21(Waf1/Cip1), during adipogenesis. J. Biol. Chem. *274*, 17088–17097.

Nakae, J., Barr, V., and Accili, D. (2000). Differential regulation of gene expression by insulin and IGF-1 receptors correlates with phosphorylation of a single amino acid residue in the forkhead transcription factor FKHR. EMBO J. *19*, 989–996.

Nakae, J., Biggs, W.I., Kitamura, T., Cavenee, W., Wright, C., Arden, K., and Accili, D. (2002). Regulation of insulin action and pancreatic beta-cell function by mutated alleles of the gene encoding forkhead transcription factor *Foxo1*. Nat. Genet. *32*, 245–253.

Nakae, J., Kitamura, T., Silver, D.L., and Accili, D. (2001). The forkhead transcription factor Foxo1 (Fkhr) confers insulin sensitivity onto glucose-6-phosphatase expression. J. Clin. Invest. *108*, 1359–1367.

Rosen, E.D., Walkey, C.J., Puigserver, P., and Spiegelman, B.M. (2000). Transcriptional regulation of adipogenesis. Genes Dev. *14*, 1293–1307.

Ross, S.E., Erickson, R.L., Gerin, I., DeRose, P.M., Bajnok, L., Longo, K.A., Misek, D.E., Kuick, R., Hanash, S.M., Atkins, K.B., et al. (2002). Microarray analyses during adipogenesis: understanding the effects of Wnt signaling on adipogenesis and the roles of liver X receptor alpha in adipocyte metabolism. Mol. Cell. Biol. *22*, 5989–5999.

Rubin, C.S., Lai, E., and Rosen, O.M. (1977). Acquisition of increased hormone sensitivity during in vitro adipocyte development. J. Biol. Chem. *252*, 3554–3557.

Sakaue, H., Ogawa, W., Matsumoto, M., Kuroda, S., Takata, M., Sugimoto, T., Spiegelman, B.M., and Kasuga, M. (1998). Posttranscriptional control of adipocyte differentiation through activation of phosphoinositide 3-kinase. J. Biol. Chem. *273*, 28945–28952.

Schreiber, E., Matthias, P., Muller, M.M., and Schaffner, W. (1989). Rapid detection of octamer binding proteins with 'mini-extracts', prepared from a small number of cells. Nucleic Acids Res. *17*, 6419.

Spiegelman, B.M., and Flier, J.S. (2001). Obesity and the regulation of energy balance. Cell *104*, 531–543.

Tang, Q.Q., and Lane, M.D. (2000). Role of C/EBP homologous protein (CHOP-10) in the programmed activation of CCAAT/enhancer-binding protein-beta during adipogenesis. Proc. Natl. Acad. Sci. USA *97*, 12446–12450.

Wang, X.Z., and Ron, D. (1996). Stress-induced phosphorylation and activation of the transcription factor CHOP (GADD153) by p38 MAP kinase. Science *272*, 1347–1349.

Wu, Z., Rosen, E.D., Brun, R., Hauser, S., Adelmant, G., Troy, A.E., McKeon, C., Darlington, G.J., and Spiegelman, B.M. (1999). Cross-regulation of C/EBP alpha and PPAR gamma controls the transcriptional pathway of adipogenesis and insulin sensitivity. Mol. Cell *3*, 151–158.